



Poly (Acrylic Acid-Acrylamide) Hydrogel for Ni(II) and Cr(III) Adsorption: Isotherm, Kinetics and Thermodynamic Studies

Reham El-Araby^{1*}, Marwa El Sayed¹, and Manal Ahmad¹

¹) Chemical Engineering and Pilot Plant Department, National Research Centre, Giza, Egypt.

Abstract

The use of a hydrogel composed of poly acrylic acid acrylamide (AA-AAm) as an adsorbent for removing nickel and chromium ions from synthetic wastewater was investigated. The effects of various factors such as pH, retention time, hydrogel dosage, and initial metal concentration on the adsorption of Ni(II) and Cr(III) were examined. Adsorption performance was evaluated using isotherms, kinetics, and thermodynamics. The results showed that the adsorption process for both metals followed a pseudo-second-order model with good correlation coefficients. The Freundlich isotherm model was found to be a better fit for the adsorption process, suggesting that both physical and chemical processes were involved in the adsorption of Ni and Cr. Thermodynamic analysis demonstrated that the adsorption process is spontaneous (negative ΔG) but endothermic (positive ΔH), indicating that heat energy is required for the adsorption process. Overall, the findings suggest that the poly AA-AAm hydrogel has excellent potential as an adsorbent for removing heavy metals from wastewater. The presence of heavy metals in wastewater is a significant environmental and health concern.

Paper type: Research paper

Keywords: Hydrogel, industrial wastewater, chromium, nickel, heavy metals removal.

Citation: El-Araby, R., M., El Sayed, and M. Ahmad "Poly (Acrylic Acid-Acrylamide) Hydrogel for Ni(II) and Cr(III) Adsorption: Isotherm, Kinetics and Thermodynamic Studies", Jordanian Journal of Engineering and Chemical Industries, Vol. 6, No.3, pp: 47-57 (2023).

Introduction

Access to safe and uncontaminated drinking water is essential for maintaining a stable and thriving society (Karimi *et al.*, 2019). However, environmental pollution resulting from the expansion of agricultural and industrial activities and the imprudent utilization of resources has increased (Ghrab *et al.*, 2018; Hosseini *et al.*, 2019). Heavy metals have been linked to a variety of human health issues, including neurological disorders, cancer, nutrient deficiencies, hormonal imbalances, respiratory and cardiovascular diseases, hair loss, osteoporosis, and damage to the liver, kidneys, and brain, even at low concentrations (Yazdani *et al.*, 2018). The introduction of hazardous elements into the environmental cycle poses a threat to life on Earth, underscoring the need to identify and remove toxic pollutants for environmental conservation (Arsiya *et al.*, 2017; Shekari, *et al.*, 2017). Water contamination is a growing global problem, and removing heavy metals from aqueous solutions is critical for pollution control. Nanotechnology has become an important tool for reducing contaminant emissions, filtering water and wastewater, eradicating pollutants, and monitoring the environment. Given the hazardous nature of heavy metals, it is crucial to eliminate these contaminants in compliance with environmental laws and regulations (El-Dessouky *et al.*, 2018).

Egypt's diverse enterprises and industrial zones generate significant amounts of industrial waste, particularly industrial wastewater, requiring water treatment within these zones to comply with permissible output levels (Osman *et al.*, 2017). Untreated discharge of this wastewater into sewage networks can cause severe contamination of groundwater, oceans, and marine life, leading to hazardous levels of sewage pollution. This is due to the difference between sewage treatment and industrial wastewater treatment. Additionally, it can cause sewage network erosion and ignores potential industrial hazards and the possibility of reusing treated water within the enterprise for manufacturing purposes (Elbltagy *et al.*, 2021).

* Corresponding author: E-mail: rehamelaraby@hotmail.com

Received on October 17, 2023.

Jordanian Journal of Engineering and Chemical Industries (JJECI), Vol.6, No.3, 2023, pp: 47-57.

ORCID: <https://orcid.org/0000-0002-3834-1156>

Accepted on November 11, 2023.

Revised: November 10, 2023.



Egypt's primary source of renewable water supplies is the Nile River, which receives around 55.5 billion cubic meter of freshwater, accounting for approximately 97% of the country's renewable water resources (El-Agha *et al.*, 2020). However, wastewater production in Egypt is approximately 2.4 billion m³/year, making recycling challenging, and most untreated wastewater is discharged into farmlands. Due to freshwater scarcity, farmers in drainage areas use this untreated wastewater as an alternative source of irrigation for various crops (SER, 2009). Additionally, like many other low-income countries, Egypt continues to release untreated wastewater due to insufficient infrastructure, technical and institutional skills, and financial resources. Furthermore, efficient wastewater treatment technologies, water quality monitoring, and control systems are limited. Consequently, numerous researchers are currently investigating the removal of heavy metals from industrial effluent (Azimi *et al.*, 2014; Ekayem *et al.*, 2021). The approaches used can be broadly categorized as chemical therapy, physical treatment, and biological treatment, based on their respective study fields and treatment mechanisms. Among these methods, adsorption is currently the most effective environmental treatment approach. Hydrogels have emerged as a cost-effective and efficient wastewater treatment technique in recent years (Sorour *et al.*, 2021). Hydrogels have emerged as a recent and cost-effective technique for treating wastewater (El Sayed, 2023). There is a growing interest in developing hydrogels with chelating groups that can rapidly and inexpensively separate and concentrate metal ions (Anah and Astrini, 2018). Crosslinked polymeric polymers with functional groups including carboxylic acid, amine, hydroxyl, amidoxime, and sulfonic acid have shown promise as complexing substances for removing metal ions from aqueous solutions. One of the main advantages of these materials is their ability to easily load and remove cations using simple chemical treatments, as well as their potential for reusability (Ekebafé *et al.*, 2012). Even small concentrations of heavy metals such as Cu²⁺ and Ni²⁺ present in industrial effluent can be harmful to humans and other living organisms. The World Health Organization has established recommended maximum levels of Cu²⁺ and Ni²⁺ in drinking water at 2.00 and 0.02-0.01mg/L, respectively (Wang *et al.*, 2017). Polyacrylamide (PAm) is commonly used as a selective adsorbent for pollution removal, either as is or grafted with functional groups (Wang *et al.*, 2018). Poly (acrylamide-co-acrylic acid) hydrogel is a hydrogel with high swelling ratio hydrophilic groups that can absorb cationic impurities in water-based solutions. This hydrogel has demonstrated excellent adsorption capability and exceptional thermal and mechanical properties, as evidenced by the synthesis of various hydrogels with different molar ratios. However, determining the optimal conditions for synthesizing the hydrogel to achieve higher swelling ratios and more efficient heavy metal removal is challenging. Moreover, the application of this hydrogel in real-world scenarios for removing heavy metals from industrial electroplating effluent requires further investigation (Shah *et al.*, 2018).

In a previous work, the synthesized poly-AAm has been characterized by extremely high distension ratios, excellent cationic methylene blue dye adsorption capacity (Alaraby and El Sayed, 2022). The current study aimed to use the synthesized poly AA-AAm hydrogel for nickel and chromium heavy metal adsorption. Batch experiments on adsorption were carried out to assess the hydrogel's adsorption characteristics towards nickel (II) and chromium (III). Isotherm, kinetic, and thermodynamic models have also been investigated to better understand the adsorption mechanism.

1 Materials and Methods

1.1 Materials

The monomers used in this study were acrylic acid (AA, MW=72.06g/gmol) and acrylamide (Am, MW=71.08g/gmol) from Baker Chemical Co., USA. The initiator was potassium persulfate (KPS, MW=248.21 g/mol) from Merck in Germany. N,N'-Methylenebisacrylamide a crosslinking agent (MBA, MW=100.1g/mol) from Merck in Germany. N,N,N',N'-Tetramethylethylenediamine catalyst (TEMED, MW=121.19 g/mol) from Merck in Germany. Nickel (II) sulfate, chromium (III) sulfate, sodium hydroxide, and nitric acid were supplied by Sigma Aldrich. Hydrochloric acid, sodium hydroxide, and ethanol were used to wash and adjust the pH. Reverse osmosis (RO) water was used in all experiments.

1.2 Preparation of AA-AAm Hydrogel

The desired amounts of AA, AAm, and MBA were weighed out. The AA and AAm were dissolved in deionized water in a glass flask. The KPS and TEMED were added to the solution and stirred continuously for 15 minutes. The solution was heated to 60°C in a water bath and stirred continuously for 2 hours. The solution was allowed to cool to room temperature and poured into a mold. The hydrogel was solidified for 24 hours and was ready to use (Alaraby and El Sayed, 2022).

1.3 Metal adsorption experiments

Batch adsorption experiments were conducted in 250mL conical flasks. The heavy metal aqueous systems contained Cr₂(SO₄)₃ and NiSO₄, each with an initial concentration ranging from 10 to 200mg/L. The poly AA-AAm hydrogel was ground and sieved to a size of 100µm before the experiments. Different amounts of hydrogel (0.2, 0.5, 1, 1.5, and 2g) were added to 100mL of the heavy metal

solutions (El Sayed, 2023). The mixture was stirred at room temperature 27, 40, and 50°C using a water bath shaker for various time intervals (20, 30, 90, 120, 180, and 270 minutes).

The adsorption amount could be calculated as follows:

$$q_t = \frac{C_0 - C_t}{m} V \quad (1)$$

$$R = \frac{C_0 - C_t}{C_0} \times 100\% \quad (2)$$

Where the quantity of heavy metal adsorbed per unit mass of the hydrogel is q_t , V , represents the volume of the aqueous solution in litres, m is the mass of the adsorbent in grams, and C_0 and C_t are respectively the initial and residual concentrations of the heavy metal in mg/L, at a given time t , Atomic Absorption Spectroscopy type Jenway3610 was used to detect the heavy metals concentration with a wavelength of 520 and 340 nm for Cr(III) and Ni(II) respectively. The pH of the solution was regulated during the experiment by utilizing pH electrodes for continuous pH monitoring. These electrodes were connected to a pH controller that could adjust the amount of acid or base added to the solution to maintain the desired pH level.

1.4 Adsorption isotherms

In this study, five equilibrium models have been investigated in order to identify the most suitable adsorption isotherm. In order to build the adsorption system to remove metal ions, the adsorbent's capacity as an adsorbent was estimated. The capacity of Cr and Ni metal ions for adsorption as well as the kind of adsorption onto the AA-AAm hydrogel were both determined by equilibrium adsorption isotherms. The adsorption performance was examined using the most generally used isotherm models, including Langmuir, Freundlich, Temkin, Dubinin-Radushkevich, and Linear Redlich-Person. The equations for the tested isotherm models, together with the assumptions of each model have been illustrated in **Table 1**.

Table 1 Isotherm adsorption linear models.

Isotherm Type	Freundlich	Langmuir	Temkin	Dubinin-Radushkevich	Redlich- Peterson
Linear Equation	$\log q_e = \log K_f + \frac{1}{n} \log C_e$	$\frac{C_e}{q_e} = \frac{1}{k_L q_{max}} + \frac{C_e}{q_{max}}$	$q_e = B \ln k_T + B \ln C_e$	$\ln q_e = \ln q_s - K_D \varepsilon^2$	$\ln \left(\frac{C_e}{q_e} \right) = \beta \ln C_e - \ln A$
Plotting Slope	$\log q_e$ vs. $\log C_e$ 1/n	C_e/q_e vs. C_e 1/q _{max}	q_e vs. $\ln C_e$ B	$\ln q_e$ vs. ε^2 -K _D	$\ln (C_e/q_e)$ vs. $\ln C_e$ β
Intercept	$\log k_f$	1/k _L q _{max}	B ln k _T	ln q _s	-ln A
Reference	Balarak <i>et al.</i> ,	Maryanti <i>et al.</i> , 2020	Maryanti <i>et al.</i> , 2020	Maryanti <i>et al.</i> , 2020	Abdul <i>et al.</i> , 2019

1.4 Kinetic adsorption

To determine the efficiency of adsorption and design sorption systems, it is essential to predict the kinetics of the chemical reaction that occurs during adsorption, considering the physicochemical properties of the adsorbent and system conditions such as temperature (Ibrahim *et al.*, 2010; Abdul *et al.*, 2019). Kinetic adsorption data may be used to understand the dynamics of the adsorption process in terms of rate constant order, and the kinetic parameters can be used to model and design the adsorption process (Georgieva *et al.*, 2020). Adsorption can occur through a variety of methods, including particle diffusion, mass transfer, and chemical reactions. Adsorption kinetics may be studied using two kinetic models: first-order and second-order. These models consider the adsorbed amounts, which may then be utilized to compute the reactor volume (Zhang *et al.*, 2022). The experimental data's adsorption process was assessed using pseudo-first order and pseudo-second-order kinetic models. The pseudo-first-order model compares the rate of adsorption at any time to the equilibrium adsorption capacity q_e , whereas the pseudo-second-order model supposes that the limiting step rate is caused by adsorbing substances that involve valence forces caused by electron exchange between the adsorbent and adsorbate species (El Sayed, 2023). The equations for the kinetic models are shown in **Table 2**. Adsorption kinetics are described using the first-order rate constant of adsorption K_1 , and the second-order rate constant of adsorption K_2 , where q_e and q_t indicate the quantities of metal ions adsorbed (mg/g) at equilibrium and time t , respectively (Georgieva *et al.*, 2020). For the adsorption kinetics experiment, a batch technique was used, where 100mg of hydrogel was immersed in 50ml of metal solutions at room temperature. The effect of contact time on the removal of both types of metals was studied using a shaker set to a constant stirring speed of

120rpm. The adsorption experiments were conducted with a contact time of 250 minutes, pH=7, and an initial metal concentration of 1000mg/L.

Table 2 Kinetics adsorption models.

Kinetic Model	General Form	Linear Form	Plotting	Parameter
First-order	$\frac{dq_t}{dt} = K_1(q_e - q_t)$	$\log((q_e - q_t)) = \log q_e - \frac{1}{2.303} k_1 t$	$\log(q_e - q_t)$ vs. (t)	$q_e = \exp(\text{intercept})$ $k_1 = -(\text{slope})$
Second-order	$\frac{dq_t}{dt} = K(q_e - q_t)^2$	$\frac{t}{q_t} = \frac{1}{k_2 q_e^2} + \frac{t}{q_e}$	t/q_t vs. (t)	$q_e = (\text{slope})^{-1}$ $k_2 = (\text{slope})^2 / \text{intercept}$

1.5 Thermodynamic adsorption

Thermodynamic studies play a crucial role in determining whether the adsorption process is spontaneous or not, as well as identifying the optimal temperature range for sorption and the nature of the sorbent and sorbate at equilibrium. The findings of thermodynamic studies can give useful information about the adsorption process and help to improve adsorption efficiency (Hosseini *et al.*, 2019). Gibbs free energy change ΔG° , enthalpy change ΔH° , and entropy change ΔS° , are addressed as they characterize the system's equilibrium to get a quick grasp of thermodynamic parameters and their influence on the sorption process (Maryanti *et al.*, 2020). The thermodynamic equilibrium coefficients obtained at various temperatures and concentrations can be used to determine the adsorption thermodynamics and verify the potential adsorption mechanisms (Ugwu *et al.*, 2020). The following Equations were used to calculate these changes during adsorption:

$$\ln Kc = \frac{\Delta S^\circ}{R} - \frac{\Delta H^\circ}{RT} \tag{3}$$

$$\Delta G^\circ = \Delta H^\circ - T \Delta S^\circ \tag{4}$$

After calculating the Langmuir constant, K_L as illustrated in the adsorption isotherm section, several thermodynamic adsorption parameters can be calculated (Pandey *et al.*, 2020). The slope of the line generated by plotting the natural logarithm of the Langmuir constant, $\ln K_L$, versus the reciprocal of the temperature, $1/T$, and fitting the data to a straight line using linear regression analysis is equal to $-\Delta H^\circ/R$, where R is the gas constant (8.314 J/mol·K). The line's intercept is equal to $\Delta S^\circ/R$. Equation 4, may be used to compute the 'Gibbs free energy' of adsorption ΔG° . The experiments were conducted at pH=7, with an adsorbent dosage of 1g/L, an initial concentration of 100mg/L of both Ni and Cr, and a shaker speed of 120 rpm at 30, 40, and 50°C for 30 minutes to evaluate the thermodynamic adsorption as the values of ΔH° , ΔS° , and ΔG° at different temperatures were calculated.

2 Results and Discussion

2.1 The effect of conditions on Ni and Cr ions removal

2.1.1 Effect of solution pH

In adsorption investigations, the pH of the adsorption material is critical. Changing the pH changes the surface charge, and degree of ionization of the adsorbent surface, which impacts adsorption capacity. As a result, the effect of pH on the adsorption of Cr(III) and Ni(II) ions has been examined throughout a pH range of 3.0 to 9.0, as shown in **Figure 1**. The findings illustrated in Fig. 1 show that the optimal operating pH for the wastewater adsorption process was at a pH ranging from 6 to 8. The findings are consistent with previous research (Ekayem *et al.*, 2021), which found that the optimal pH for metal ion adsorption is between 5 and 7. These results may be attributed to that at low pH levels, the solution is highly protonated resulting in a high positive charge density on the hydrogel's surface. An excess of

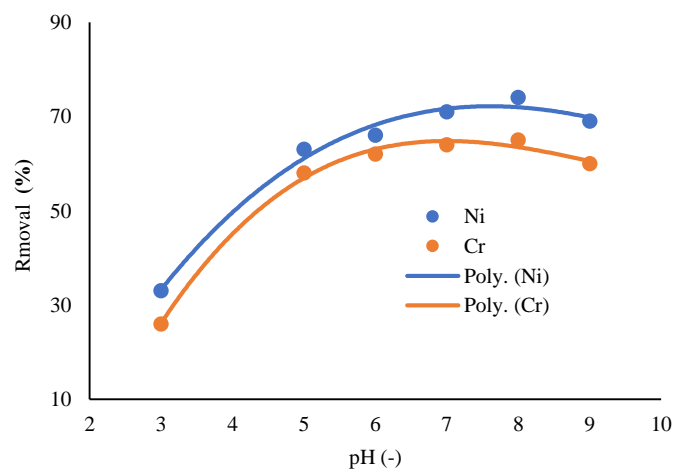


Fig. 1 Effect of pH on the removal of Cr and Ni ions ($C_i=100$ mg/L, $T=25^\circ\text{C}$, Time=1 hr).

protons H^+ in the solution competes for adsorption sites and repels the metal cations causing the active sites in the hydrogel to become protonated and the adsorption capacity to be insufficient. While, at higher pH values, the solution is less protonated due to the predominance of negatively charged hydroxide ions. The surface of the hydrogel develops a high negative charge density and the deprotonation of carboxyl groups was accelerated as the pH increased by changing of carboxyl groups ($-COOH$) of AA onto the hydrogel to become carboxylates ($-COO^-$). Therefore, it exhibited strong electrostatic attraction for Cr(III) and Ni(II) and led to the attraction of more metal ions and therefore increased adsorption capacity. The removal was 74% and 65% for nickel and chromium, respectively at pH=8.

2.1.2 Effect of contact time

To ensure complete adsorption, an equilibrium between the solute in the solution and the adsorbent must be established, which requires a specific amount of time for the equilibrium interactions to take place. This time is referred to as the contact time, and it is critical to achieve optimal adsorption (Khayyun and Mseer, 2019). Several studies have investigated the effect of contact time on adsorption and have found that the rate of metal adsorption increases with time until an optimum value is reached, after which no further metal removal occurs (Maryanti *et al.*, 2020). The quantity of metal ion adsorbed at the equilibrium contact time may be used to calculate the adsorbent's maximal adsorption capacity under operational circumstances. In adsorption investigations, determining the contact time necessary for the adsorbate-adsorbent system to attain equilibrium is an important parameter (Bayuo *et al.*, 2018; Du *et al.*, 2021). In this study, the effect of contact time and the equilibrium points of adsorption of Cr(III) and Ni(II) from an aqueous solution were determined at an initial concentration of 100 mg/L and a temperature of 27°C. **Figure 2** demonstrates that the adsorption of metal ions increased as the contact time increased, and equilibrium was established after 60 minutes of shaking. The percentage of metal removal did not show a significant change after this point and remained constant until 4 hours. The initial uptake of metal ions was rapid within the first 60 minutes and then levelled off for the remainder of the study period. This observation can be explained by the quick occupancy of the adsorbent's surface's restricted number of accessible adsorption sites. As a result of these findings, the shaking time was adjusted at 60 minutes. The initial adsorption capacity was found to be high due to the availability of more active sites' on the adsorbent's surface, which ultimately became saturated (Yao *et al.*, 2023).

2.1.3 Effect of adsorbent dosage

A dosage study is a critical metric in adsorption investigations since it determines an adsorbent's capacity for a specific starting concentration of metal ion solution (Maryanti *et al.*, 2020). **Figure 3** depicts the effect of 'adsorbent dose on Cr(III) and Ni(II) ion' adsorption. To identify the best dose for removing the most Cr(III) and Ni(II) from an aqueous solution with an initial concentration of 100 mg/L, adsorbent dosages of 0.25, 0.50, 0.75, 1.00, and 1.50g/L were examined. As expected, increasing the adsorbent dose (hydrogel) increased the removal efficiency for a given initial metal concentration, as more surface area or adsorption sites are provided for a fixed initial metal ion concentration. This increase can also be attributed to metal ion binding to the surface functional groups of the hydrogel. The findings of this study are consistent with those of a previous study (Hosseini *et al.*, 2019). After a 1-hour contact time at 27°C and pH=7, the removal percentage increased from 52 to 82% for C (III) and from 69 to 86% for Ni(II). Based on these results, a dosage of 1.00g/L was proposed for the remaining experiments. Beyond this optimal dosage, the adsorbent dosage had no significant effect on the removal efficiency.

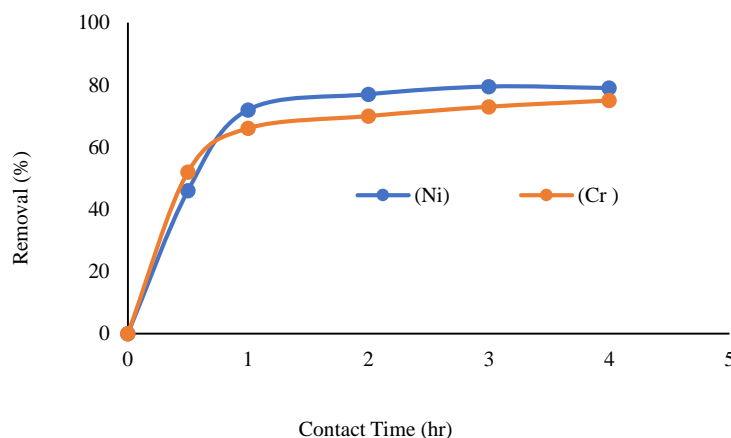


Fig. 2 Effect of contact time on the removal of Cr and Ni ions ($C_i=100\text{g/L}$, $T=25^\circ\text{C}$, $\text{pH}=7$).

2.1.4 Effect of initial concentration

The initial concentration of heavy metals in a solution has a direct impact on the removal percentage (Farag *et al.*, 2018). The adsorption rate of Ni and Cr ions decreases as their initial concentration increases. The results depicted in **Figure 4** indicate that as the concentration of Ni and Cr ions increased from 25 to 150mg/L, the percentage removal decreased from 92% to 59% and from 87% to 50% for Ni and Cr, respectively. The results demonstrate that the removal effectiveness of Cr and Ni is inversely proportional to their original concentration. This discovery implies that 'the adsorbents have a limited number of active sites that become saturated at high concentrations as the number of ions competing for reaction with the functional groups on the hydrogel's surface' grows with initial metal ion concentration. Similarly, raising the concentration of metal ions increases the interaction between these ions and the adsorbent, which speeds up the process (Ugwu *et al.*, 2020). A prior investigation on the elimination of hexavalent chromium using sawdust found similar results to the current study (Abdul *et al.*, 2019). Furthermore, research on heavy metal removal (Ibrahim *et al.*, 2010) discovered that when the concentration of metal ions increases, the removal efficiency falls, which is similar to the current study's findings.

2.1.5 Determination of adsorption isotherm model

To describe the equilibrium data of heavy metal adsorption onto AA-AAm hydrogel, various adsorption isotherm models were employed. The Langmuir, Freundlich, Temkin, Dubinin Radushkevick, and Redlich-Peterson isotherm linear models were used to characterize the adsorption equilibrium and determine the optimal correlations for the equilibrium curves. Batch adsorption experiments were conducted on 0.1g of AA-AAm hydrogel under pH=7 conditions, with a 1-hour contact time, and initial Ni and Cr concentrations of 1000mg/L. The results of the adsorption experiments were then used to create the isotherm curves, as shown in **Figure 5**. The correlation coefficient obtained from the assessment of the isotherms was used as a suitable criterion for determining the most appropriate model (Ekebafe *et al.*, 2012). The results of the adsorption isotherm models' showed that the correlation coefficients of the Langmuir, Freundlich, Temkin, Dubinin Radushkevick, and Redlich-Peterson models differed. Among the five isotherm models, the Freundlich isotherm was the most appropriate for describing the adsorption of Ni and Cr on AA-AAm hydrogel, as the correlation coefficients of Freundlich were the largest for both Ni and Cr, exceeding 0.98 in **Figures (5-a)**, and **(5-b)**. These findings indicate that the adsorption of Ni and Cr through AA-AAm hydrogel follows the Freundlich model, suggesting chemisorption and multilayer adsorption as the most likely mechanisms. The results are consistent with a previous study (Anah and Astrini, 2018), where the Freundlich model was found to be the optimal isotherm for Ni(II) adsorption on modified carboxymethyl cellulose hydrogel absorbers.

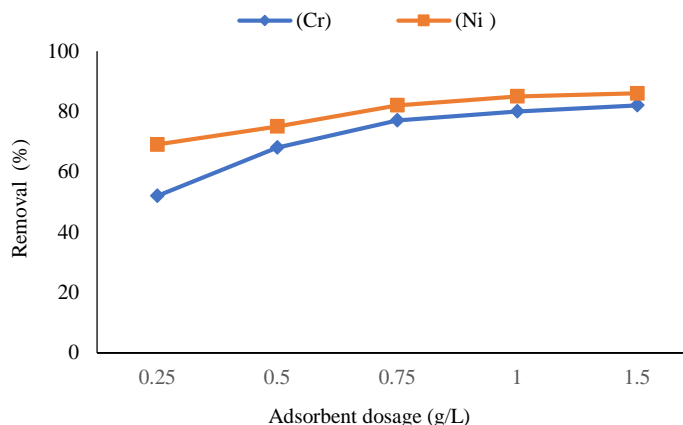


Fig. 3 Effect of adsorbent dosage on the removal of Cr and Ni ions ($C_i=100$ mg/L, $T=27^\circ\text{C}$, pH=7, Time=1hr).

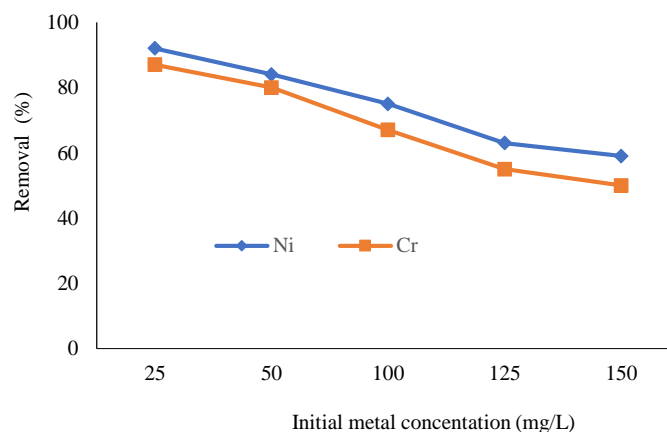
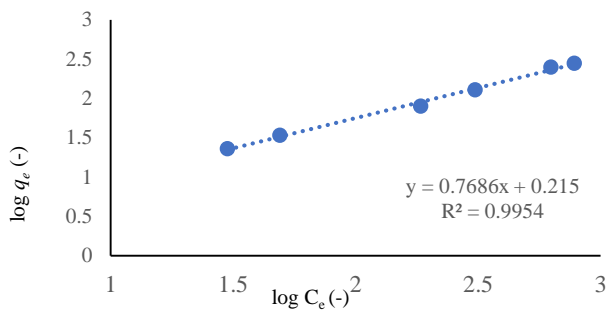
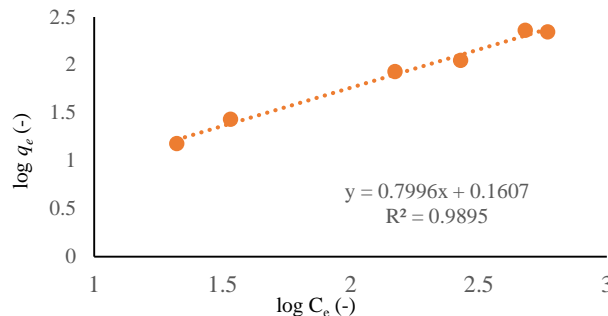


Fig. 4 Effect of initial concentration of Cr and Ni Ions on the removal ($T=27^\circ\text{C}$, pH=7, Time=1hr).

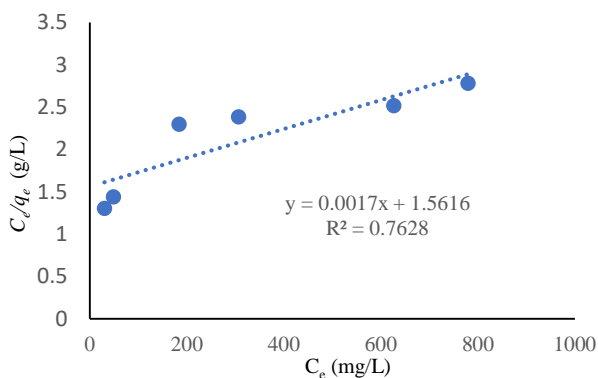
The Freundlich equation is often used to describe adsorption data over a limited concentration range and applies to both homogeneous and highly heterogeneous surfaces, indicating multi-layer adsorption (Yao *et al.*, 2023). The Freundlich constants K_F and $1/n$ were 1.64 (mg/g (L/mg)^{1/n}) and 0.77 respectively. Values of $1/n$ less than unity suggest significant adsorption at low concentrations but a less significant increase in the amount adsorbed with concentration at higher concentrations, and vice versa. Additionally, as $n > 1$, it implies that for less heterogeneous surfaces, active sites with the highest binding energies would be used first,



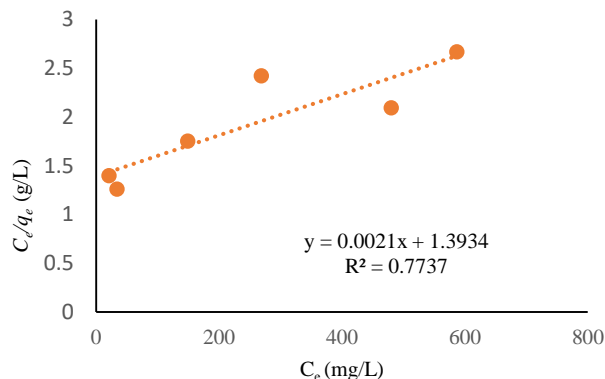
(a) The Freundlich adsorption isotherm of Ni.



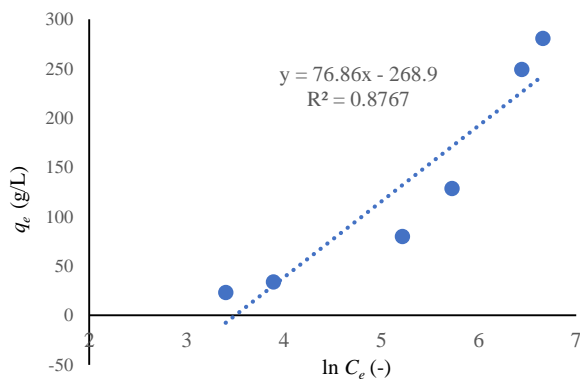
(b) The Freundlich adsorption isotherm of Cr.



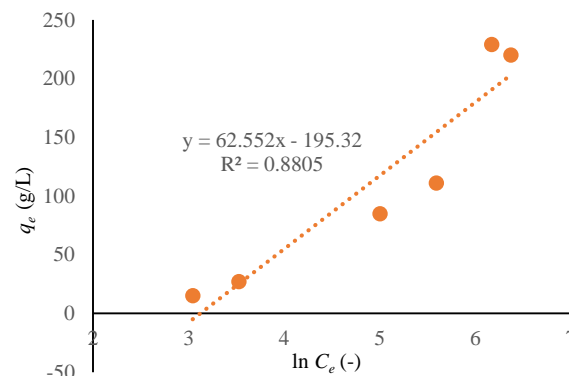
(c) The Langmuir adsorption isotherm of Ni



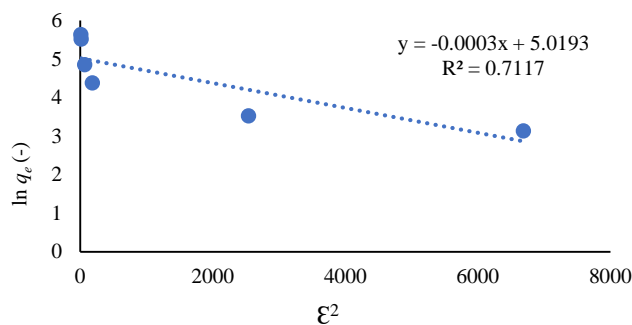
(d) The Langmuir adsorption isotherm of Cr.



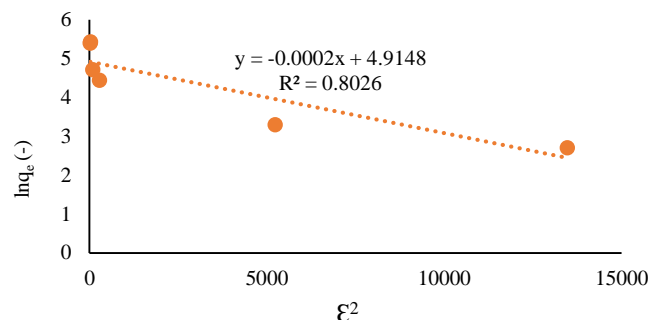
(e) The Temkin adsorption isotherm of Ni.



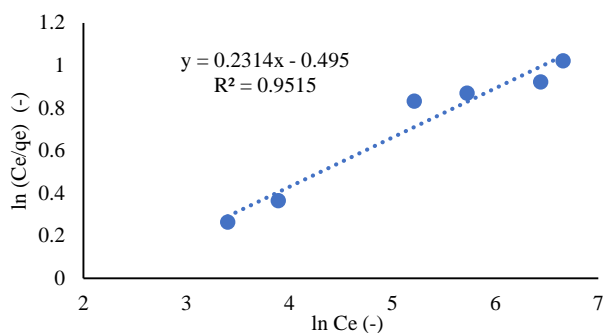
(f) The Temkin adsorption isotherm of Cr.



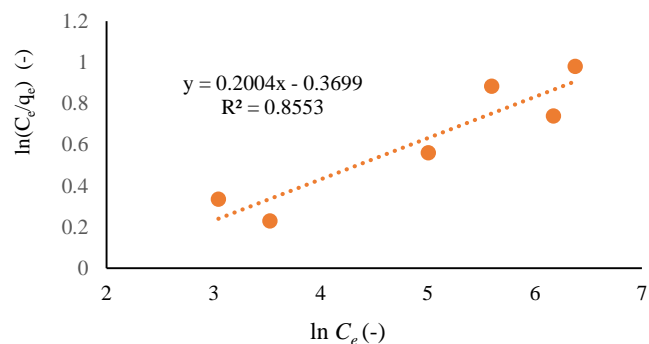
(g) The Dubinin-Radushkevich adsorption isotherm of Ni.



(h) The Dubinin-Radushkevich adsorption isotherm of Cr.



(i) The Linear Redlich-Peterson adsorption isotherm of Ni.



(j) The Linear Redlich-Peterson Adsorption Isotherm of Cr.

Fig. 5 Adsorption isotherm.

followed by weaker sites for more heterogeneous surfaces (Farag *et al.*, 2018). A value of n between 2 and 10 is an indicator of good adsorption (Salim *et al.*, 2020). The calculated n values for the adsorption of Ni and Cr were 1.3 and 1.25mg/L, respectively, indicating good adsorption efficiency for both metals. High R^2 values indicate good agreement with the Freundlich model, and n indicates the favorability of the adsorption process. Since all n values fall between 1 and 10, the adsorbent hydrogel has exhibited favourable adsorption (Anah and Astrini, 2018).

It is worth noting that the Redlich-Peterson isotherm competes with the Freundlich isotherm for Ni, with a correlation coefficient of 0.9515 compared to 0.9954 for Freundlich, as shown in **Figures (5-i)** and **(5-j)**. The q_m , which represents the maximum adsorption capacity according to the Langmuir isotherm, is 588.23mg/g for Ni and 476.2mg/g for Cr. These results suggest that AA-AAM hydrogel has a higher maximum adsorption capacity for Ni than Cr, according to the Langmuir isotherm. The findings showed that the adsorption of Ni and Cr did not fit well with other isotherm models, as the R^2 values for both metals were less than 0.90.

2.1.6 Evaluation of adsorption kinetics

To determine the kinetics of adsorption of Cr(III) and Ni(II) onto AA-AAM hydrogel, the pseudo-first-order and second-order models were applied to the experimental data. The regression correlation coefficient obtained from the pseudo-first-order kinetic graph was found to be low ($R^2=0.5137$ and 0.5434) for Ni and Cr, respectively, as shown in **Table 3**, indicating that the pseudo-first-order kinetic model did not apply to the experimental data of Cr(III) and Ni (II) adsorption on the hydrogel. However, the application of the second-order kinetic model by plotting t/q_t vs t yielded high regression correlation coefficients for both Cr (III) and Ni (II) adsorption on the hydrogel, indicating that the two heavy metal ions were absorbed using second-order kinetics. The linear coefficients and constants of the kinetic models are shown in Table 3. For Ni and Cr ions, the correlation coefficient for the pseudo-second-order kinetic model was higher than that for 'the pseudo-first-order model ($R^2=0.9981$ and $R^2=0.9993$), indicating that the adsorption perfectly complies with and is controlled by the pseudo-second-order model. The slope and 'intercept of the t/q_t against t graphs may be used to get the q_e and k_2 values of the pseudo-second-order kinetic model. Figs. (5-e) and (5-f) show kinetic graphs of t/q_t vs t for

Ni(II) and Cr (III) adsorption at 27°C. The correlation coefficient R^2 had an extraordinarily high value (>0.99), as shown in Table 3, and its predicted equilibrium adsorption capacity q_e was consistent with the experimental findings. These findings indicate that the pseudo-second-order adsorption mechanism predominates and that the overall rate constant of each adsorption process appears to be governed by the chemical adsorption process (Sorour *et al.*, 2021). Similar to covalent forces and ion exchanges, the K_2 constant was utilized to characterise chemisorption including valency forces via electron sharing or exchange between the hydrogel and heavy metal ions (Yao *et al.*, 2023). As indicated in Table 3, the K_2 constant verified that the adsorption rate of Ni(II) onto the produced hydrogel was quicker than the adsorption rate of Cr(III). Additionally, the theoretical q_e values calculated from the pseudo-second-order kinetic model agreed with the experimental q_e values.

Table 3 Adsorption kinetics parameters results.

Metal	Pseudo-First-Order	Pseudo-Second-Order
Ni	$R^2=0.5081$	$R^2=0.9991$
	$K_1=0.0011515$ (1/min)	$K_2=0.0018$ (g/mg·min.)
	q_e (calculated)=244 (mg/g)	q_e (calculated)=84 (mg/g)
Cr	$R^2=0.611$	$R^2=0.9995$
	$K_1=0.0011515$ (1/min)	$K_2=0.00129$ (g/mg·min.)
	q_e (calculated)=281 (mg/g)	q_e (calculated)=80 (mg/g)

2.1.7 Adsorption Thermodynamic Parameter Determination

Table 4 presented the values of the thermodynamic parameters ΔG , ΔH , and ΔS for Ni and Cr adsorption on the AA-AAm hydrogel. The findings suggested that the adsorption process for Ni and Cr was endothermic and impacted by temperature changes. The ΔG values in Table 4 were negative and decreased as the temperature increased, indicating that the adsorption of Ni and Cr ions onto AA-AAm hydrogel was feasible and spontaneous and that increasing temperature was beneficial to adsorption, consistent with the trend of q_e/C_e , versus the positive ΔH values suggested that the adsorption mechanism of Ni (II) and Cr (III) onto AA-AAm hydrogel was an endothermic process, as increasing temperature resulted in an increase in the maximum adsorption capacity and was controlled by physical and chemical adsorption mechanisms (Yao *et al.*, 2023). Positive ΔS values indicated an increase in disorder on the solid-liquid surface throughout the adsorption process, resulting in a minor change in adsorbent structure and adsorbate and rendering adsorption irreversible (Farag *et al.*, 2018). These results confirm the interaction of Ni⁺² and Cr⁺³ metal ions with the reactive sites on the surface of the prepared hydrogel and suggest that the complexation of heavy metal ions enhances the adsorption of additional free ions. Consequently, heavy metal ions cause an increase in entropy.

Table 4 Thermodynamic parameters for adsorption of Ni (II) and Cr (III)

Metal	Temperature (K)	ΔG° (kJ/mol)	ΔH° (kJ/mol)	ΔS° (J/mol·K)
Ni	300	-1.1	22.9	0.08
	313	-2.14		
	323	-2.94		
Cr	300	-0.7	11.3	0.04
	313	-1.22		
	323	-1.62		

Conclusions

In this study, a polyacrylic acid-acrylamide (AA-AAm) hydrogel was prepared, and the effects of pH, hydrogel dose, and initial Ni and Cr concentrations on the removal percentage of the two heavy metals from simulated synthetic wastewater were evaluated. From the findings, it was concluded that: the optimal operating pH for the wastewater adsorption process was a pH ranging from 6 to 8. Furthermore, metal adsorption increased with contact time and achieved equilibrium after 60 minutes of shaking. Furthermore, the percentage removal of metals did not exhibit a significant change after this point and remained constant for up to four hours. An increase in the adsorbent dose (hydrogel) led to an improvement in removal efficiency for a given initial metal concentration. After one hour of contact time at 27°C and pH 7, the percentage of elimination rose considerably for both Cr (III) and Ni (II). The percentage of elimination rose for Cr (III) from 52% to 82% and for Ni (II) from 69% to 86%. As the initial Ni and Cr ion concentration rose from 25 to 150mg/L, the elimination percentage of these metals dropped. The percentage elimination of Ni reduced from 92% to 59% and Cr from 87% to 50%. This shows that with increasing starting metal concentrations, the adsorption process becomes less efficient. The adsorption kinetics of metal ions onto the hydrogel material agreed very well with a pseudo-

second-order model. In other words, the rate of adsorption was dependent on the second power of the concentration of metal ions in solution, indicating that the adsorption process was predominantly controlled by chemical adsorption. The adsorption process of metal ions onto the hydrogel material followed the Freundlich isotherm model. This indicates that the adsorption process was heterogeneous, with adsorption capacity increasing with metal ion concentration in solution until saturation occurred. The adsorption process of metal ions onto the hydrogel material was both endothermic and spontaneous. The 'positive value of ΔH° ' indicated that the process required the input of heat energy, while the 'negative value of ΔG° ' indicated that the process was energetically favorable and feasible. This suggests that the adsorption process was thermodynamically driven and could occur spontaneously in the studied conditions.

Acknowledgment

The authors wish to thank Department of Chemical Engineering and pilot plant, National Research Centre, Giza, Egypt.

Nomenclature

A	=Redlich- Peterson isotherm constant	[L/mg]
AA	=Acrylic Acid	[-]
AAm	=Acrylamide	[-]
B	=Constant related to the heat of adsorption	[mg/g]
β	= β : Linear Redlich-Person exponential value range from 0 to 1.	[-]
C_e	=Equilibrium concentration of metal ions in solution	[mg/L]
Cr (III)	=Cromium	[-]
ΔG°	=Gibbs free energy change	[kJ/mol]
ΔH°	=Enthalpy change	[kJ/mol]
ΔS°	=Adsorption entropy	[J/mol·K]
k_f	=Freundlich constant related with solid adsorption capacity	[mgg ⁻¹ (L/mg) ^{1/n}]
V	=Volume	[L]
K_D	=Dubinin–Radushkevich isotherm constant	[mol ² /kJ ²]
K_D	=Dubinin–Radushkevich isotherm constant	[mol ² /kJ ²]
k_L	=Langmuir constant related to a free energy of adsorption	[mg/g]
KPS	=Potassium persulphate	[-]
k_T	=Equilibrium binding constant corresponding to the maximum binding energy	[L/g]
MBA	=Methylene Bis Acrylamide	[-]
n	=Freundlich constants related to adsorption intensity	[-]
Ni (II)	=Nikle	[-]
q_e	=Amount of metals adsorbed at the equilibrium concentration	(mg/g)
q_{max}	=Langmuir maximum adsorption capacity	[mg/g]
q_s	=Theoretical isotherm saturation capacity	[mg/g]
TEMED	=N,N,N',N'-Tetramethylethylenediamine	[-]

References

- Abdul, S., Muhammad, S., Ibrahim, A., and B., Ibrahim "Thermodynamic Study on the Adsorptive Removal of Cr (VI) and Ni (II) Metal Ions Using Schiff Base as Adsorbent", *Moroccan J. of Chem.*, **7**, 7-3, (2019).
- Alaraby, R., and M., El Sayed "Methylene Blue Cationic Dye Removal using AA-Am Hydrogel as An Efficient Adsorbent", *Egyptian J. of Chem.*; **65**, (2022).
- Anah, L., and N., Astrini, "Isotherm adsorption studies of Ni (II) ion removal from aqueous solutions by modified carboxymethyl cellulose hydrogel", *InIOP Conference Series: Earth and Envi. Sci.*, **160**, 01, (2018).
- Arsiya, F., Sayadi M., and S., Sobhani "Arsenic (III) adsorption using palladium nanoparticles from aqueous solution", *J. of Water and Env. Nanotechnology.*, **2**, 166-173, (2017).
- Azimi, A., Azari A., and M., Rezakazemi "Ansarpour M. Removal of heavy metals from industrial wastewaters: a review", *Chem. Bio. Eng. Reviews*, **4**, 37-59, (2017).
- Balarak, D., Mostafapour, F., Azarpira, and H., Joghataei "Langmuir, Freundlich, Temkin and Dubinin–radushkevich isotherms studies of equilibrium sorption of ampicilin unto montmorillonite nanoparticles", *J. of Pharm. Res. Int.*, **2**, 1-9, (2017).
- Bayuo, J., Pelig-Ba, B., and M. A., Abukari "Isotherm modeling of lead (II) adsorption from aqueous solution using groundnut shell as a low-cost adsorbent", *IOSR J. Appl. Chem.*, **11**, 18-23, (2018).
- Du, X., Cheng, Y., Liu, Z., Yin, H., Wu, T., Huo, L., and C., Shu "CO₂ and CH₄ adsorption on different rank coals: A thermodynamics study of surface potential Gibbs free energy change and entropy loss", *Fuel*, 283,118886, (2021).
- Ekebaf, O., Ogebeifun, E., and E., Okieimen "Removal of heavy metals from aqueous media using native cassava starch hydrogel", *African J. of Env. Sci. and Tech.*, **6**, 275-282, (2012).

- Ekrayem, A., Alhwaige, A., Elhrari, W., and M., Amer "Removal of lead (II) ions from water using chitosan/polyester crosslinked spheres derived from chitosan and glycerol-based polyester", *J. of Env. Chem. Eng.*, **9**, 106628, (2021).
- El Sayed, M. "Production of Polymer Hydrogel Composites and Their Applications", *J. of Polymers and the Env.*, **15**, 1-25, (2023).
- El-Agha, E., Molle, F., Rap, E., El Bialy, M., and A., El-Hassan "Drainage water salinity and quality across nested scales in the Nile Delta of Egypt", *Env. Sci. and Pollution Res.*, **27**, 32239-50, (2020).
- Elbltagy, H., Elbasiouny, H., Almuhamady, A., and H., Gamal El-Dein, "Low Cost and Eco-Friendly Removal of Toxic Heavy Metals from Industrial Wastewater", *Egyptian J. of Soil Sci.*, **61**, 219-229, (2021).
- El-Dessouky, I., Ibrahim, H., El-Masry, H., El-deen, S., Sami, M., Moustafa, E., and M., Mabrouk "Removal of Cs⁺ and Co²⁺ ions from aqueous solutions using poly (acrylamide-acrylic acid)/kaolin composite prepared by gamma radiation", *Appl. Clay Sci.*, **151**, 73-80, (2018).
- Farag, A., M., Sokker, H., H., Zayed, E., M., Eldien, F., A., and N., M., Abd Alrahman "Removal of hazardous pollutants using bifunctional hydrogel obtained from modified starch by grafting copolymerization", *Int. J. of Biol. Macromolecules*, **120**, 2188-2199, (2018).
- Georgieva, V., G., Gonsalvesh, L., and M., P., Tavlieva "Thermodynamics and kinetics of the removal of nickel (II) ions from aqueous solutions by biochar adsorbent made from agro-waste walnut shells", *J. of Molecular Liquids*, **312**, 112788, (2020).
- Ghrab, S., Mefteh, S., Medhioub, M., and M., Benzina "Adsorption of nickel (II) and chromium (III) from aqueous phases on raw smectite: kinetic and thermodynamic studies", *Arabian J. of Geosciences*, **11**, 1-9, (2018).
- Hosseini, R., Sayadi, M., H., and H., Shekari "Adsorption of nickel and chromium from aqueous solutions using copper oxide nanoparticles: adsorption isotherms, kinetic modeling, and thermodynamic studies", *Avicenna J. of Env. Health Eng.*, **6**, 66-74, (2019).
- Ibrahim, S., Fatimah, I., Ang, H., M., and S., Wang "Adsorption of anionic dyes in aqueous solution using chemically modified barley straw", *Water Sci. and Tech.*, **62**, 1177-1182, (2010).
- Karimi, P., Javanshir, S., Sayadi, M., H., and H., Arabya "Arsenic removal from mining effluents using plant-mediated, green-synthesized iron nanoparticles", *Processes*, **7**, 1-19, (2019).
- Khayyun, T., S., and A., H., Mseer, "Comparison of the experimental results with the Langmuir and Freundlich models for copper removal on limestone adsorbent", *Applied Water Sci.*, **9**, 1-8, (2019).
- Maryanti, R., I., Nandiyanto, A., B., Manullang, T., I., Hufad, A., and S., Sunardi "Adsorption of dye on carbon microparticles: physicochemical properties during adsorption, adsorption isotherm and education for students with special needs", *Sains Malaysiana*, **49**, 2949-2960, (2020).
- Osman, H., E., Abdel-Hamed, E., W., Al-Juhani, W., S., Al-Marouai, Y., A., and M., El-Morsy, "Bioaccumulation and human health risk assessment of heavy metals in food crops irrigated with freshwater and treated wastewater: a case study in Southern Cairo, Egypt", *Env. Sci. and Pollution Res.*, **28**, 50217-50229, (2017).
- Pandey, S., Fosso-Kankeu, E., Spiro, M., J., Waanders, F., Kumar, N., Ray, S., S., Kim, J., and M., Kang "Equilibrium, kinetic, and thermodynamic studies of lead ion adsorption from mine wastewater onto MoS₂-clinoptilolite composite", *Materials Today Chem.*, **18**, 100376, (2020).
- Salim, N., A., Puteh, M., H., Yusoff, A., R., Abdullah, N., H., Fulazzaky, M., A., Rudie, M.A., and N., A., Zainuddin "Adsorption isotherms and kinetics of phosphate on waste mussel shell" *Malaysian J. of Fund. and Appl. Sci.*, **16**, 393-399, (2020).
- SER, State of the Environment Report - Ministry of State for Environmental Affairs-Egyptian Environmental Affairs Agency, (2009).
- Shah, L., A., Khan, M., Javed, R., Sayed, M., Khan, M., S., Khan, A., and M., Ullah "Superabsorbent polymer hydrogels with good thermal and mechanical properties for removal of selected heavy metal ions", *J. of Cleaner Production*, **201**, 78-87, (2018).
- Shekari, H., Sayadi, M., H., Rezaei, M., R., and A., Allahresani "Synthesis of nickel ferrite/titanium oxide magnetic nanocomposite and its use to remove hexavalent chromium from aqueous solutions", *Surfaces and Interfaces*, **8**, 199-205, (2017).
- Sorour, M., H., Hani, H., A., Shaalan, H., F., El Sayed, M., M., and M., A., El-Toukhy "Adsorption isotherms and kinetics pertinent to modified composite hydrogel adsorbents adopted for heavy metals removal", *Int. J. of Appl. Sci. and Eng.*, **18**, 1-12, (2021).
- Ugwu, E., I., Tursunov, O., Kodirov, D., Shaker, L., M., Al-Amieri, A., A., Yangibaeva, I., and F., Shavkarov "Adsorption mechanisms for heavy metal removal using low cost adsorbents: A review", *INOP Conference Series: Earth and Env. Sci.*, **614**, 1-13, (2020).
- Wang, F., Pan, Y., Cai, P., Guo, T., and H., Xiao "Single and binary adsorption of heavy metal ions from aqueous solutions using sugarcane cellulose-based adsorbent", *Bioresour. Tech.*, **241**, 482-490, (2017).
- Wang, X., Zhou, J., Zhao, S., Chen, X., and Y., Yu "Synergistic effect of adsorption and visible-light photocatalysis for organic pollutant removal over BiVO₄/carbon sphere nanocomposites", *Appl. Surface Sci.*, **453**, 394-404, (2018).
- Yao, J., Yang, H., Zuo, D., Xu, J., and H., Zhang "Facile preparation and adsorption behavior studies of poly (acrylic acid)-based hydrogels reinforced by hydrogen bonds for methylene blue dye", *J. of Polymers and the Env.*, **31**, 552-564, (2023).
- Yazdani, A., Sayadi, M., and A., Heidari "Green biosynthesis of palladium oxide nanoparticles using dictyota indica seaweed and its application for adsorption", *J. of Water and Env. Nanotechnology*, **6**, 338-356, (2018).
- Zhang, H., Li, G., W., Feng, W., and Z., Yao "Cu (II) Adsorption from Aqueous Solution onto Poly (Acrylic Acid/Chestnut Shell Pigment) Hydrogel", *Water*, **14**, 1-13, (2022).